

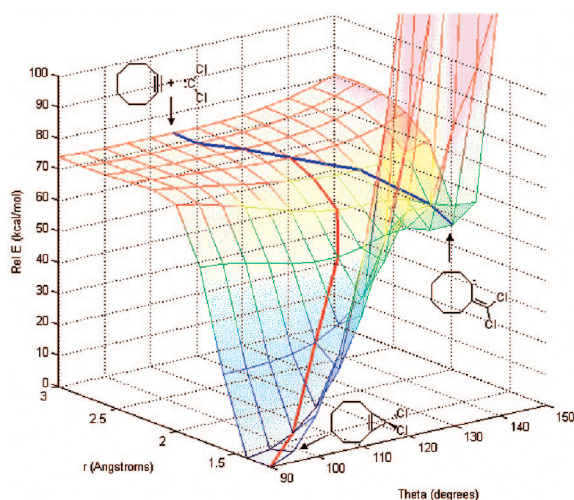
A Computational Study of Chlorocarbene Additions to Cyclooctyne

Xiao Yu Mo, Sarah E. Bernard, Marina Khrapunovich, and Dina C. Merrer*

Department of Chemistry, Barnard College, 3009 Broadway, New York, New York 10027

dmerrer@barnard.edu

Received August 4, 2008



Dichloro- and phenylchlorocarbene (CCl_2 and PhCCl) add to cyclooctyne via a barrierless process (MP2/6-311+G*, B3LYP/6-311+G*, B3LYP/6-31G*) to yield the expected corresponding cyclopropene adducts. A three-dimensional potential energy surface (PES) for CCl_2 addition to cyclooctyne (B3LYP/6-31G*) shows the formation of the cyclopropene product and also possible formation of a vinylcarbene. Residing in a shallow energy well, the vinylcarbene easily rearranges to the cyclopropene product, or to an exocyclic vinyl bicyclo[3.3.0]octane. Although the calculated three-dimensional PES indicates possible dynamic control of the cyclooctyne–chlorocarbene system through the putative formation of a vinylcarbene (in addition to the expected cyclopropene), additional calculations and preliminary experimental work show paths through the vinylcarbene to be unlikely. If the additions of chlorocarbenes to cyclooctyne are controlled by reaction dynamics, we predict that the vast majority of the reactions proceed via traditional carbene cycloaddition with only a very minor amount of products formed from the alternative pathway.

Introduction

Our previous computational investigations of the additions of dichlorocarbenes to strained π systems have shown the transition state for initial carbene addition to lead to multiple reaction paths and therefore multiple products.^{1,2} Specifically, CCl_2 adds to cyclopropene to yield both bicyclobutane and butadiene from the same transition state via a concerted process (eq 1).¹ Similarly, benzocyclopropene and CX_2 ($\text{X} = \text{Cl}, \text{Br}$) react regioselectively to produce dihalobenzocyclobutenes, whereby initial CX_2 addition may generate the benzocyclobutenes directly or through xylylene intermediates, and the transition state to both benzocyclobutenes and xylylenes is the same (eq 2).²

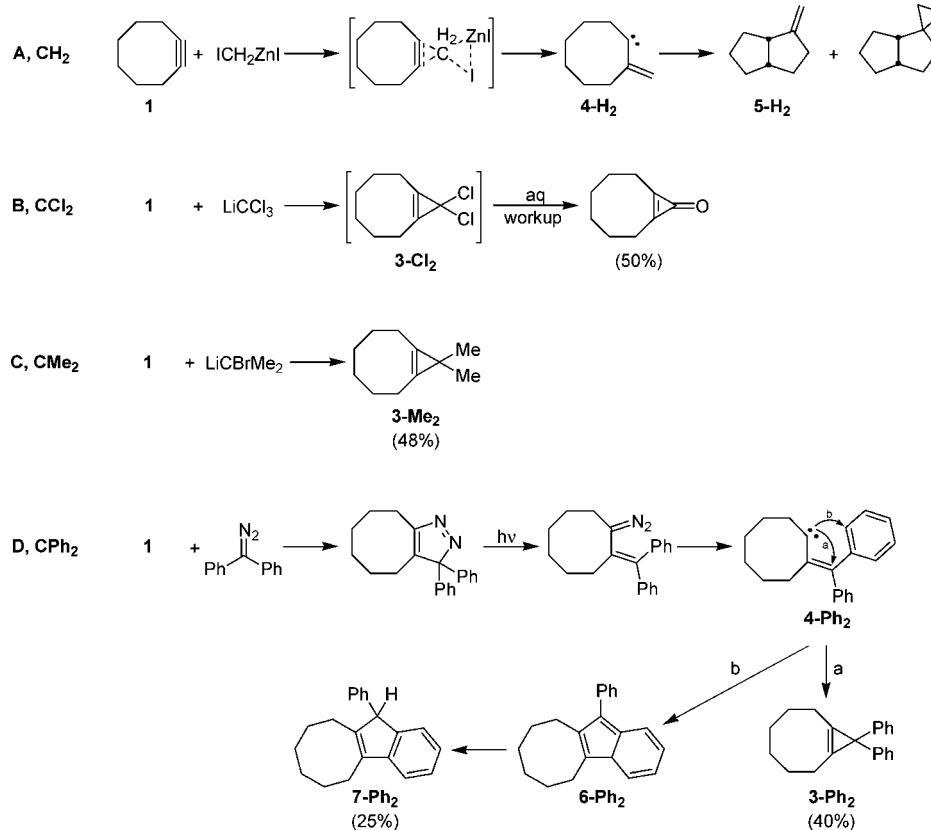
The phenomenon of a single transition state leading to multiple products on potential energy surfaces (PESs) containing flat reaction plateaus suggests possible dynamic control of such

(3) (a) Carpenter, B. K. In *Reactive Intermediate Chemistry*; Moss, R. A., Platz, M. S., Jones, M., Jr., Eds.; Wiley: Hoboken, NJ, pp 925–960. (b) Carpenter, B. K. *J. Phys. Org. Chem.* **2003**, *16*, 858. (c) Carpenter, B. K. *Angew. Chem., Int. Ed.* **1998**, *37*, 3340.

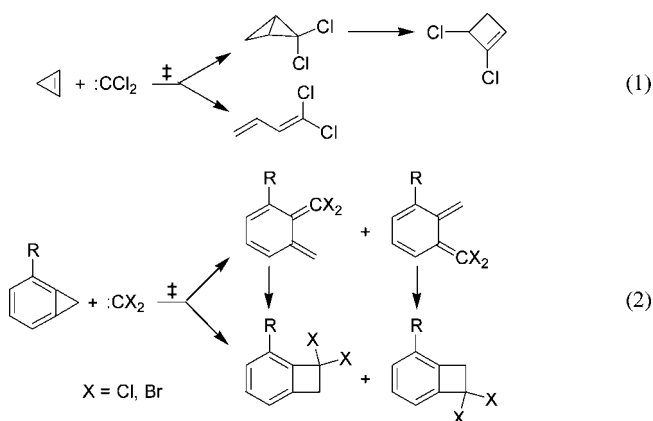
(4) (a) Bolton, K.; Hase, W. L.; Doubleday, C., Jr. *J. Phys. Chem. B* **1999**, *103*, 3691. (b) Doubleday, C., Jr.; Bolton, K.; Hase, W. L. *J. Phys. Chem. A* **1998**, *102*, 3648. (c) Doubleday, C., Jr.; Bolton, K.; Hase, W. L. *J. Am. Chem. Soc.* **1997**, *119*, 5251. (d) Hrovat, D. A.; Fang, S.; Borden, W. T.; Carpenter, B. K. *J. Am. Chem. Soc.* **1997**, *119*, 5253.

(1) Merrer, D. C.; Rablen, P. R. *J. Org. Chem.* **2005**, *70*, 1630–1635.

(2) Khrapunovich, M.; Zelenova, E.; Seu, L.; Sabo, A. N.; Flaherty, A.; Merrer, D. C. *J. Org. Chem.* **2007**, *72*, 7574–7580.

SCHEME 1. Wittig and Hutchison's Mechanisms for Carbene (or Carbenoid) Additions to Cyclooctyne (**1**)¹¹

reactions.^{1–6} Our overarching interest in the role dynamic effects may play in intermolecular singlet carbene addition reactions to strained C–C π systems has led us to investigate computationally and experimentally dihalocarbene (CCl₂, CBr₂) and phenylhalocarbene (PhCCl, PhCBr) additions to cyclooctyne (**1**). Herein are reported our theoretical results for CCl₂ and PhCCl (**2**; RCCl, R = Cl, Ph) additions to **1**. Our experimental studies are ongoing and will be reported in due course.



Cyclooctyne (**1**) is the smallest isolable cycloalkyne, with a C≡C–C alkynyl bond angle of 163°;⁷ it is air sensitive and rearranges and polymerizes easily.⁸ Its 1,3-dipolar cycloaddition with phenyl azide to produce the corresponding triazole was reported to proceed “like an explosion,”^{8b} attesting to **1**'s ring strain of 16 kcal/mol.⁹ The geometric constraints of cyclooctyne account for its inherent reactivity, which can be used to promote reactions that are otherwise difficult or impossible for unstrained alkynes. For instance, Bertozzi and co-workers have utilized the reactivity of **1** to promote a [3 + 2] azide–alkyne cycloaddition in order to selectively modify biomolecules and living cells without apparent physiological damage.¹⁰

Carbene additions to cyclooctyne were first investigated by Wittig and Hutchison.¹¹ They reacted **1** with CH₂, CPh₂, CCl₂, and CMe₂ (or their respective carbenoids) via various carbene precursors; their results and mechanisms are shown in Scheme 1 and are described below.

As shown in Scheme 1, the mechanisms proposed by Wittig and Hutchison for carbene(oid) addition to cyclooctyne vary with the type, source, and method of carbene generation.¹¹ Methylene carbenoid generated from iodomethylzinc iodide reacts with **1** to give carbene **4-H₂**, which undergoes transannular

(7) Meier, H.; Petersen, H.; Kolshorn, H. *Chem. Ber.* **1980**, *113*, 2398.

(8) (a) Blomquist, A. T.; Liu, L. H. *J. Am. Chem. Soc.* **1953**, *75*, 2153. (b) Wittig, G.; Krebs, A. *Chem. Ber.* **1961**, *94*, 3260.

(9) (a) Turner, R.; Jarrett, A. D.; Goebel, P.; Mallon, B. J. *J. Am. Chem. Soc.* **1972**, *95*, 790–792. (b) Roberts, J. D.; Caserio, M. C. *Basic Principles of Organic Chemistry*, 2nd ed.; W. A. Benjamin: Menlo Park, CA, p 475.

(10) (a) Agard, N. J.; Prescher, J. A.; Bertozzi, C. R. *J. Am. Chem. Soc.* **2004**, *126*, 15046–15047. (b) Agard, N. J.; Baskin, J. M.; Prescher, J. A.; Lo, A.; Bertozzi, C. R. *ACS Chem. Biol.* **2006**, *1*, 644–648.

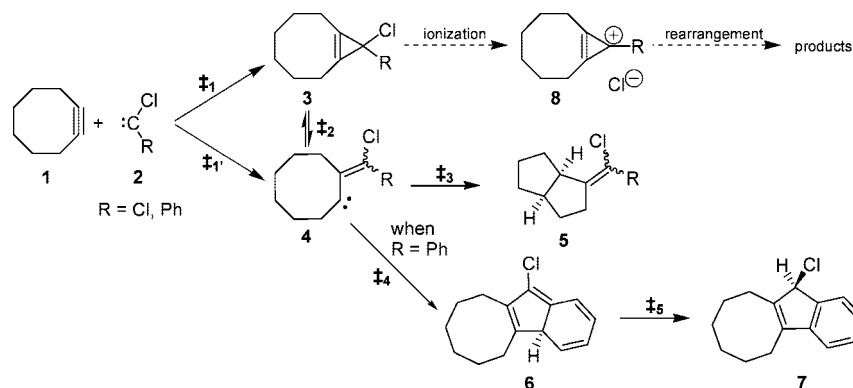
(11) Wittig, G.; Hutchison, J. J. *Liebigs Ann. Chem.* **1970**, *741*, 79–88.

(12) Anslyn, E. V.; Dougherty, D. A. *Modern Physical Organic Chemistry*; University Science: Sausalito, CA, 2006; p 111.

(5) (a) Baldwin, J. E. *Chem. Rev.* **2003**, *103*, 1197. (b) Doubleday, C.; Li, G.; Hase, W. L. *Phys. Chem. Chem. Phys.* **2002**, *4*, 304. (c) Doubleday, C. *J. Phys. Chem. A* **2001**, *105*, 6333. (d) Doubleday, C.; Nendel, M.; Houk, K. N.; Thweatt, D.; Page, M. *J. Am. Chem. Soc.* **1999**, *121*, 4720.

(6) (a) Doubleday, C.; Suhrada, C. P.; Houk, K. N. *J. Am. Chem. Soc.* **2006**, *128*, 90. (b) Doering, W. v. E.; Cheng, X.; Lee, K.; Lin, Z. *J. Am. Chem. Soc.* **2002**, *124*, 11642. (c) Baldwin, J. E.; Keliher, E. J. *J. Am. Chem. Soc.* **2002**, *124*, 380.

SCHEME 2. Proposed Pathways of RCCl (2) Addition to Cyclooctyne (1)



insertion to bicyclo[3.3.0]octane derivative **5-H₂** (Scheme 1, eq A). Excess CH₂ carbenoid, in turn, reacts with **5-H₂** to also produce a spirodecane. α -Halolithium carbenoids LiCCl₃ and LiCBrMe₂ add to **1** to produce cyclopropenes **3-Cl₂** and **3-Me₂**, respectively (Scheme 1, eqs B and C). Finally, reactions of **1** and diphenyldiazomethane produce a stable pyrazoline which, when irradiated, isomerizes to the analogous diazo compound (Scheme 1, eq D). The diazo compound eliminates N₂ to yield vinyl carbene **4-Ph₂**, subsequently inserting into either the adjacent double bond to form cyclopropene **3-Ph₂** (path a), or into a phenyl C–H bond (**6-Ph₂**; path b) followed by rearrangement to indene **7-Ph₂**.

Using Wittig and Hutchison's findings¹¹ as a framework, we have proposed a mechanism for the addition of chlorocarbenes **2** to cyclooctyne (Scheme 2). We have calculated the potential energy surface (PES) of this mechanistic scheme via density functional (B3LYP) and ab initio (MP2) methods to examine its plausibility. Of particular interest are the structures of the proposed transition states of initial carbene addition to **1**, i.e., ‡₁ and ‡_{1'}. As stated above, previous studies on CCl₂ addition to cyclopropene¹ and to benzocyclopropene² have shown multiple products to derive from a single transition state, suggesting control by dynamic effects. The calculations described below show that the additions of chlorocarbenes **2** to **1** are barrierless, and also may be controlled by reaction dynamics. Our computed three-dimensional PES shows **1** + **2** to yield the expected cyclopropene adduct (**3**), as well as the alternative reaction route through vinylcarbene **4**. Additional calculations and our preliminary experimental results lead us to believe that very few, if any, of the reactions proceed through **4**. Indeed, if **4** is formed at all, it rapidly rearranges either to **3** or to other products (i.e., **5**, **7**).

Results and Discussion

Initial Chlorocarbene (2) Additions to Cyclooctyne (1): Attempted Calculation of Transition States ‡₁ and ‡_{1'}. In conjunction with ongoing experimental product studies of CX₂ and PhCX (X = Br, Cl) additions to cyclooctyne in our group,¹³ we have calculated the potential energy surfaces (PESs) for the reactions of cyclooctyne with CCl₂ (**2-Cl₂**) at B3LYP/6-311+G* and MP2/6-311+G* and with PhCCl at

B3LYP/6-31G*, according to the proposed mechanistic pathways shown in Scheme 2.

The most interesting, and challenging, part of computing these PESs is the initial addition of RCCl, **2** (R = Cl, Ph), to cyclooctyne. Dichlorocarbene additions to unstrained¹⁴ and strained^{1,2} alkenes have been calculated to proceed with near-negligible activation barriers, i.e., 0–2 kcal/mol. Moss and co-workers determined an experimental activation energy of 2 kcal/mol for PhCCl + 3-hexyne in isoctane solvent.¹⁵ Therefore, a priori, we expected only slight barriers, if any, for **1** + **2**.

We followed previous methods^{1,2,14} used for calculating the bimolecular reaction of CCl₂ with alkenes for this study: RCCl (**2**) was set at a fixed distance, *r*, between the carbene carbon and the midpoint of cyclooctyne's π system, optimizing the geometry from effective infinity (*r* = 3.5 Å) to *r* = 1.0 Å. Carbene **2** was positioned at two different starting geometries with respect to **1**: (a) endo to the ring (above) and (b) exo to the ring (from the side) (Figure 1) These two approach geometries were selected to account for **1**'s relatively cylindrical π system so as not to bias carbene addition.



FIGURE 1. Initial geometry of approach of carbenes RCCl (**2**) to cyclooctyne (**1**): (a) endo and (b) exo (R = Cl, Ph). Distance *r* is the distance from the carbene carbon to the midpoint of **1**'s π system and is varied by 1.0–3.5 Å.

At MP2/6-311+G* and B3LYP/6-311+G*, CCl₂ addition to cyclooctyne proceeds via a barrierless process (Figure 2). Similar results are obtained when the 6-31G* basis set is used. The reaction coordinate, *E*_{rel} vs *r* for **1** + CCl₂ is similar, regardless of the starting position of the carbene, either endo or exo to **1** (Supporting Information, Figure S1). As *r* decreases, the overall energy of the system also decreases, at first gradually at *r* = 3.5–2.2 Å, and more dramatically from *r* = 2.0 Å into a potential well at *r* = 1.3 Å. The structure at the bottom of these potential wells corresponds to cyclopropene **3-Cl₂**.

The geometry of CCl₂ addition to **1** follows a concerted asynchronous path, analogous to that calculated for CCl₂ addition to 1-butene¹⁴ and to cyclopropene.¹ To illustrate this

(13) Napolitano, D.; Suski, K.; Schloss, J.; Khrapunovich, M.; Merrer, D. C. Unpublished results. We have also determined the product of **1** + CX₂ (X = Cl, Br) not to be **3-X₂**, as the ¹³C NMR spectrum shows nine nonequivalent carbons. However, we believe that **3-X₂** undergoes ionization and rearrangement to other possible products.

(14) Keating, A. E.; Merrigan, S. R.; Singleton, D. A.; Houk, K. N. *J. Am. Chem. Soc.* **1999**, *121*, 3933–3938.

(15) Moss, R. A.; Jang, E. G.; Ho, G.-J. *J. Phys. Org. Chem.* **1990**, *3*, 760–763.

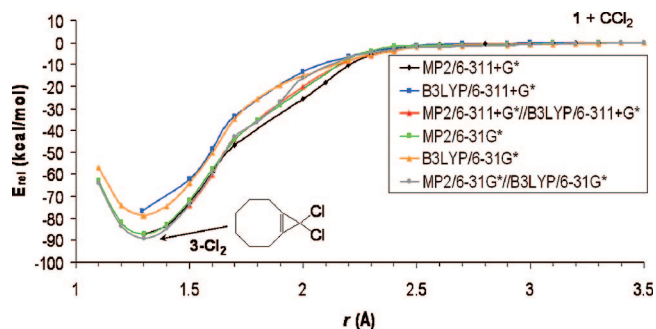


FIGURE 2. Reaction coordinate of relative electronic energies (uncorrected) for **1** + CCl₂ calculated in the gas phase, where r is the distance between the carbene carbon and the midpoint of the alkyne (endo approach).

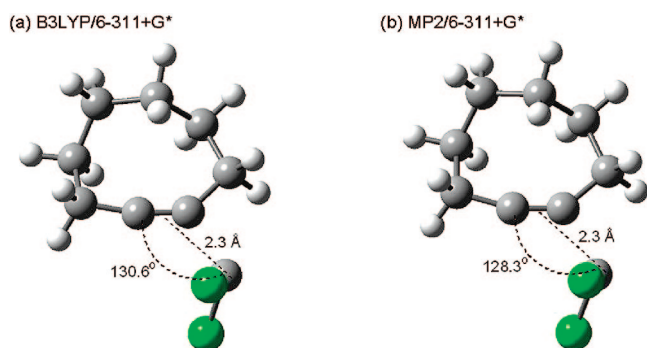


FIGURE 3. Optimized geometries for CCl₂ + cyclooctyne (**1**) at $r = 2.3$ Å: (a) B3LYP/6-311+G*, (b) MP2/6-311+G*.

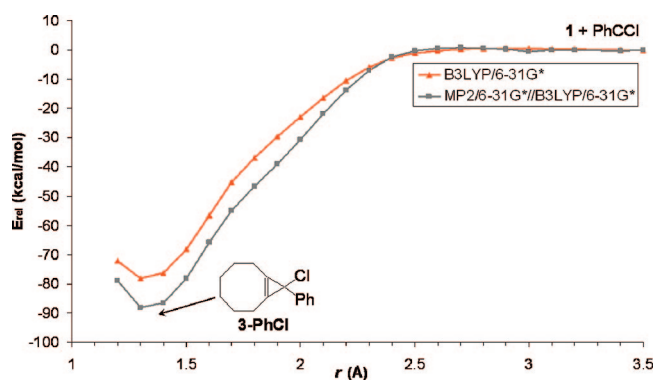


FIGURE 4. Reaction coordinate of relative electronic energies (uncorrected) for PhCCl addition to **1** calculated in the gas phase, where r is the distance between the carbene carbon and the midpoint of the alkyne.

asymmetric addition, the structure of CCl₂ + **1** at $r = 2.3$ Å is depicted in Figure 3.

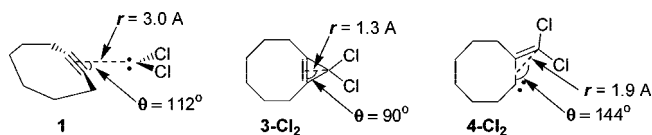
For phenylchlorocarbene (PhCCl) addition to cyclooctyne, calculation of the reaction coordinate E_{rel} vs r , as defined above, at B3LYP/6-31G* and MP2/6-31G*/B3LYP/6-31G* show slight barriers to addition (i.e., ‡₁) when the energies are uncorrected for ZPE (Figure 4): $E_a = 0.7$ kcal/mol ($r = 2.8$ Å) at B3LYP/6-31G* and $E_a = 0.8$ kcal/mol ($r = 2.7$ Å) at MP2/6-31G*/B3LYP/6-31G*. As was the case for **1** + CCl₂, phenylchlorocarbene addition to **1** produces corresponding cyclopropene adduct **3-PhCl** as a minimum, 77 kcal/mol more stable than the starting materials. These near-negligible activation energies are comparable to those previously calculated for CCl₂ addition to each of 1-butene,¹⁴ 1,2-disubstituted cyclopropenes,¹ and aryl-substituted benzocyclopropenes² (i.e., $E_a =$

0–2 kcal/mol). However, after ZPE corrections¹⁶ of these two sets of calculated energies for **1** + PhCCl, the minimal activation barriers disappear, such that the process of **1** + PhCCl becomes barrierless, as that described above for **1** + CCl₂. Therefore, we conclude that the reaction of each of CCl₂ and PhCCl with cyclooctyne proceeds initially without any barrier to addition.

Because our previous investigations of CCl₂ addition to cyclopropene and to benzocyclopropene yielded PESs characterized by common transition states for initial carbene addition to the π substrate resulting in multiple reaction paths, we explored the possibility that, in addition to cyclopropene product **3**, **1** + **2** may directly produce carbene **4** as well. We deemed this alternate pathway to carbene **4** particularly promising because of the fact that additions of **1** + **2** are calculated to be barrierless, in contrast with the slight barriers to addition for CCl₂ to cyclopropenyl systems.^{1,2} Therefore, because dichlorocarbene additions to cyclopropenes have minimal barriers and these reactions diverge to different products from a common transition state, we believed that **1** + **2**, which has no barrier, may be even more likely to proceed via alternative paths, i.e., to **4**.

We were concerned that the methods used above, i.e., E_{rel} vs r (exo and endo approach), inadvertently bypassed the possible formation of **4** from **1** + **2**. To ensure that we did not overlook the production of **4** due to our selected computational technique, we computed a three-dimensional PES at B3LYP/6-31G* of **1** + CCl₂. B3LYP/6-31G* was selected because it provided results comparable to those obtained with a larger basis set and at the MP2 level of theory (cf. Figure 2). We defined two relevant coordinates for the PES: the distance, r , between the carbene center and center of the cyclooctyne π system (as previously), and the angle, θ , from the carbene center to the midpoint of the cyclooctyne triple bond to one of the alkynyl carbons (Figure 5). The former coordinate decreases from effective infinity to ~ 1.3 Å in cyclopropene **3-Cl₂** and ~ 1.9 Å in carbene **4-Cl₂**. The angle coordinate begins at a value of 112° for the separated cyclooctyne and CCl₂, decreases to 90° in **3-Cl₂**, and expands to 144° in **4-Cl₂**. For these PES calculations, $r = 1.2$ – 3.0 Å in 0.2-Å increments and $\theta = 90$ – 150° in 5° increments.¹⁷ The resulting surface is shown in Figure 5.

Overlaid as the black path on the 3D surface in Figure 5a are the points from the two-dimensional reaction coordinate (E_{rel} vs r , B3LYP/6-31G*) of **1** + CCl₂ in Figure 2. The angles θ were abstracted from each of the optimized geometries from every point in the B3LYP/6-31G* reaction coordinate in Figure 2 to obtain the black trace. Overlaid as the red and blue paths on the 3D surface in Figure 5b are proposed paths that, if followed, would result in the more direct formation of cyclopropene **3-Cl₂** (red) and carbene **4-Cl₂** (blue). We have not yet calculated direct trajectories for this system but plan to do so in a future study.



The 3D PES shows that both **3-Cl₂** and **4-Cl₂** may be formed as a result of **1** + CCl₂. The surface also shows that carbene

(16) (a) Merrick, J. P.; Moran, D.; Radom, L. *J. Phys. Chem.* **2007**, *111*, 11683–11700. (b) Scott, A. P.; Radom, L. *J. Phys. Chem.* **1996**, *100*, 16502.

(17) All points were optimized fully at B3LYP/6-31G*, except for the point at $r = 1.8$ Å, $\theta = 140^\circ$. Despite numerous attempts to optimize this structure using several different techniques, only a partially optimized structure was able to be obtained.

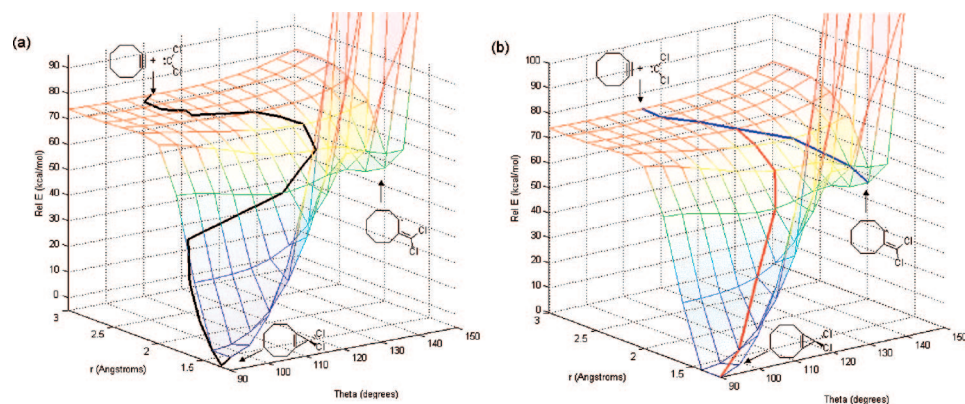


FIGURE 5. Three-dimensional PES of **1** + CCl₂ at B3LYP/6-31G*. (a) Black trace is overlay of two-dimensional reaction coordinate from Figure 2. (b) Blue and red traces are proposed paths for the formation of **3-Cl₂** and **4-Cl₂**.

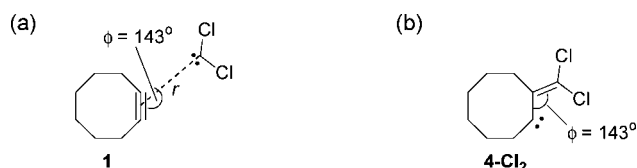


FIGURE 6. Geometry of approach of CCl₂ to cyclooctyne (**1**), where r is the distance from the carbene carbon to the midpoint of **1**'s π system, and $\phi = 143^\circ$: (a) separate species **1** + CCl₂, (b) **4-Cl₂**.

4-Cl₂ resides in a very shallow energy minimum, with easy ring closure to **3-Cl₂** ($E_a = 6\text{--}8$ kcal/mol, see below). As will be described, if **4** is indeed formed during this reaction, it can easily ring close to **3** ($E_a = 0\text{--}1$ kcal/mol for **4-PhCl** \rightarrow **3-PhCl**), or rearrange to other products (i.e., **5**, **7-PhCl**) without much difficulty ($E_a \leq 1$ kcal/mol). Therefore, the topology of the 3D PES suggests that reaction dynamics may control the fate of the additions of chlorocarbenes (or at least CCl₂) with cyclooctyne). That said, we will offer additional computational and some preliminary experimental evidence to the contrary: i.e., we believe that most reactions of **1** + **2** proceed by traditional carbene cycloaddition (to **3**), and that if any of the reactions proceed through the alternative pathway containing carbene **4**, these reactions are very few in number.

To investigate further whether or not **1** + **2** produce carbene **4** directly, preliminary calculations were conducted on the **1** + CCl₂ system at HF/6-31G*. Calculation of a restricted-geometry reaction coordinate, E_{rel} vs r was conducted where the carbene approach angle, ϕ , was held constant at 143° to promote the formation of **4-Cl₂** (Figure 6) and $r = 1.1\text{--}3.5$ Å.¹⁸ The 143° angle was selected because this value corresponds to the same angle in the optimized geometry of **4-Cl₂**.

When the carbene approach angle ϕ is maintained at 143° , the energy minimum for the reaction coordinate E_{rel} vs r occurs at $r = 2.0$ Å, the structure of which corresponds not surprisingly to **4-Cl₂**.¹⁸ On this geometrically restricted reaction coordinate, an energy maximum was computed at $r = 2.4$ Å. This partially optimized transition-state structure, obtained by holding r constant at 2.4 Å and ϕ at 143° , was subsequently fully optimized (at HF/6-31G*), i.e., the previous constants r and ϕ were permitted to fully optimize. Under these conditions, a structure corresponding to cyclopropene **3-Cl₂** resulted, rather than carbene **4-Cl₂**. These exploratory results indicate that **4-Cl₂**

likely resides in a shallow well on the PES of **1** + CCl₂, and that the rearrangement of **4-Cl₂** to **3-Cl₂** is facile. The rearrangement **4-Cl₂** \rightarrow **3-Cl₂** will be discussed in more detail below.

To be completely certain that we did not overlook a possible transition state (i.e., \ddagger_1') for the reaction **1** + CCl₂ \rightarrow \ddagger_1' \rightarrow **4-Cl₂**, we also calculated this possible reaction in the reverse direction: i.e., **4-Cl₂** \rightarrow \ddagger_1' \rightarrow **1** + CCl₂. The reverse reaction was computed by lengthening the C=C alkene bond of **4-Cl₂** in 0.1 Å increments from 1.3 to 2.1-Å at B3LYP/6-31G*.¹⁸ In **4-Cl₂**, C=C = 1.35 Å. Upon elongating the C=C bond, the structure eclipses an energy maximum at C=C = 1.40 Å that is close in structure to \ddagger_2 , and then settles into a minimum corresponding to **3-Cl₂** (when C=C = 1.50 Å). As C=C is stretched further, the structures retrace their steps, reverting to the original starting point, **4-Cl₂**, when C=C > 1.80 Å. Figure 7 shows B3LYP/6-31G*-optimized geometries at three different points in the reverse reaction: C=C = 1.35 Å, corresponding to **4-Cl₂**; C=C = 1.40 Å, corresponding to a transition state (\ddagger_2) between **4-Cl₂** and **3-Cl₂**; and C=C = 1.50 Å, corresponding to **3-Cl₂**.

Our experimental investigations thus far on the reaction of **1** with CX₂ (X = Br, Cl, generated from CHX₃ and ⁻OtBu) show evidence of a dihalogenated product.¹³ This product has yet to be fully identified and characterized, but we have determined it not to be **5-Cl₂** (when X = Cl), by comparison with an authentic sample of **5-Cl₂**.¹⁹ According to our proposed mechanism (Scheme 2), **5-Cl₂** would have been generated from carbene **4-Cl₂**. Therefore, since **5-Cl₂** is not an experimental product of **1** + CCl₂, our experimental results are consistent with the calculations presented here that show reactions proceeding through carbene **4-Cl₂** to be unfavorable. In accord with these findings, we also have found two yet-to-be-characterized monohalogenated products to result from the irradiation of phenylhalodiazirines (X = Br, Cl) with **1** in benzene solvent. Synthesis of an authentic sample of **7-PhCl**²⁰ has shown this product not to be produced experimentally, which is also consistent with our experimental results that the pathway of **1** + **2** does not proceed to **4** (and its products).

In summary, the three-dimensional PES for **1** + **2** suggests the possible formation of carbene **4**. However, our two-dimensional reaction coordinate calculations, E_{rel} vs r , for both the forward reaction, **1** + CCl₂, and our attempted reverse reaction coordinate, **4-Cl₂** \rightarrow **1** + CCl₂, resulted in no transition

(18) The reaction coordinates for **1** + CCl₂ \rightarrow **4-Cl₂** at HF/6-31G*, **4-Cl₂** \rightarrow \ddagger_1' \rightarrow **1** + CCl₂, and **4** \rightarrow **4'** \rightarrow **5** are included as Figures S2–4 in the Supporting Information.

(19) Dowbenko, R. *Tetrahedron* **1964**, *20*, 1843–1858.

(20) Karmarkar, P. G.; Chinchore, V. R.; Wadia, M. S. *Synthesis* **1981**, *3*, 228–229.

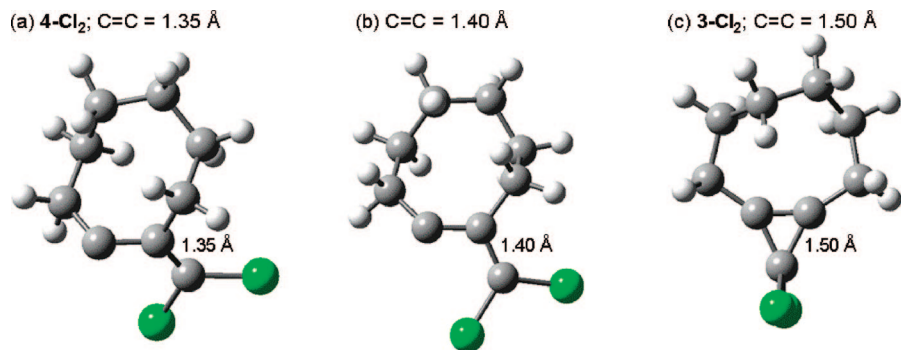


FIGURE 7. B3LYP/6-31G*-optimized geometries for the simulated reverse reaction, $4\text{-Cl}_2 \rightarrow \ddagger_1' \rightarrow 1 + \text{CCl}_2$, where $\text{C}=\text{C}$ is varied from 1.3 to 2.1 Å: (a) $\text{C}=\text{C} = 1.35$ Å, corresponding to 4-Cl_2 ; (b) $\text{C}=\text{C} = 1.40$ Å, corresponding to a transition state between 4-Cl_2 and 3-Cl_2 ; and (c) $\text{C}=\text{C} = 1.50$ Å, corresponding to 3-Cl_2 .

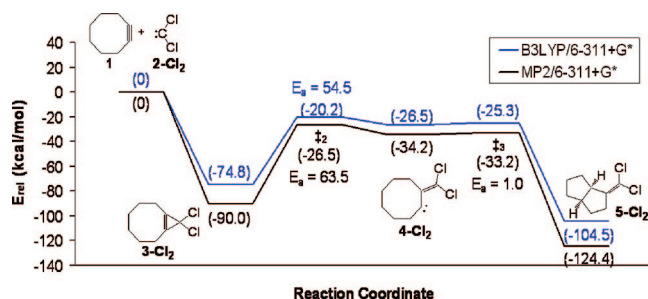


FIGURE 8. Complete PES for $1 + \text{CCl}_2$ at B3LYP/6-311+G* and MP2/6-311+G*. Relative energies are in kcal/mol and are ZPE-corrected.¹⁶

state corresponding to \ddagger_1' . Rather, carbene 4-Cl_2 converts easily to cyclopropene 3-Cl_2 . Therefore, calculations for the forward and reverse reactions of $1 + \text{CCl}_2 \rightarrow 4\text{-Cl}_2$ show carbene 4-Cl_2 not to be a stable intermediate product of dichlorocarbene addition to cyclooctyne. Our preliminary experimental findings similarly show that products originating from 4 are not formed. Therefore, if 4-Cl_2 is formed at all during the addition of dichlorocarbene to cyclooctyne, it is formed in an energetically unstable state, readily rearranging to the more stable cyclopropene 3-Cl_2 as the species progress downhill on the overall PES of this system. The tenuous stability and ready rearrangements of 4-Cl_2 (and 4-PhCl) will be described in more detail below.

We took into account the results of our unsuccessful search for a pathway connecting $1 + \text{CCl}_2$ to carbene 4-Cl_2 when considering the possible reaction $1 + \text{PhCCl} \rightarrow 4\text{-PhCl}$ as well. As detailed in the next section, the *E*- and *Z*-isomers of 4-PhCl both reside in very shallow minima, energy wells similar to that of 4-Cl_2 . Carbenes *E*- 4-PhCl and *Z*- 4-PhCl revert to 3-PhCl with $E_a = 0.4$ and 1.2 kcal/mol, respectively (B3LYP/6-31G*). Therefore, by comparison to the dichlorocarbene case, we believe the formation of 4-PhCl directly from $1 + \text{PhCCl}$ to also be unlikely.

Calculation of the Remainder of the PESs of Cyclooctyne (1) + Chlorocarbenes 2. The complete PESs for the proposed mechanisms of CCl_2 and of PhCCl addition to 1 , as depicted in Scheme 2, are shown in Figures 8 and 9, respectively. We determined above that $1 + 2$ likely forms cyclopropene 3 as the major product, and that carbene 4 may form from initial cyclooctyne-carbene addition, but 4 may subsequently easily convert to 3 : ZPE-corrected activation barriers for $4 \rightarrow 3$ range from 0.4 to 7.7 kcal/mol for $4 \rightarrow 3$ (vide infra). If the forward process shown in Scheme 2, i.e., $3 \rightarrow 4$, were to occur, it would mean that a secondary energy barrier of 49–63 kcal/

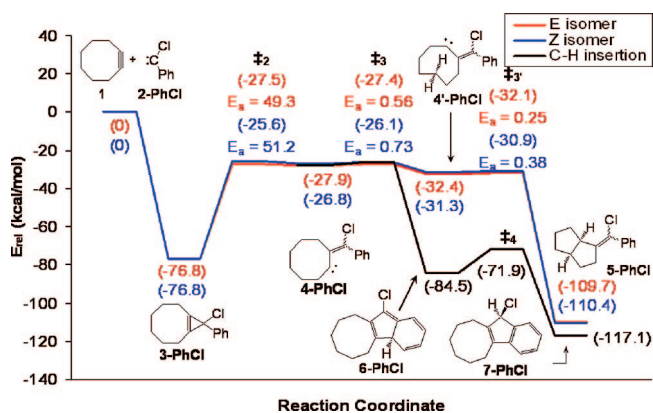


FIGURE 9. Complete PES for $1 + \text{PhCCl}$ at B3LYP/6-31G*. Relative energies are in kcal/mol and are ZPE-corrected.¹⁶

mol would need to be surmounted. Significant secondary energy barriers of 26–45 kcal/mol have been calculated to be overcome for very exothermic reactions ($\Delta H \sim < -100$ kcal/mol) with little initial activation barriers, e.g., $^1\text{CH}_2$ addition to propyne²¹ and CCl_2 addition to benzocyclopropene.² In both of these cases, reaction dynamics are believed to play a role in product formation. While we believe that dynamics may result in the formation of carbene 4 from initial cyclooctyne-carbene addition, the barrier from cyclopropene 3 to 4 appears to be too substantial to be surmounted (Figures 5, 8, and 9). Furthermore, condensed-phase reactions, particularly ones involving at least 11 heavy atoms, like here, can more readily dissipate collisional energy, thereby decreasing (or eliminating altogether) dynamic control of this reaction.³

Recall also that our experimental investigations thus far on the reaction of 1 with 2 show no evidence of products originating from carbene 4 .¹³ That said, in the unlikely event that carbene 4 indeed forms, 4 is expected to be short-lived, residing in a relatively shallow potential energy well: if 4 does not convert to 3 , it may alternatively undergo transannular C–H insertion to bicyclo[3.3.0]octane derivative 5 ($E_a = 0.6$ – 2.4 kcal/mol). With a larger basis set (B3LYP/6-311+G*, MP2/6-311+G*), 4-Cl_2 was found to rearrange to 5-Cl_2 directly via \ddagger_3 . However, at B3LYP/6-31G*, $4 \rightarrow 5$ was slightly more complex. For the dichloro derivative and both *E*- and *Z*-phenylchloro analogues, the conformation of carbene 4 as originally computed turns out not to be the conformational isomer that leads to 5 . All attempted quadratic synchronous transit methods for calculation of \ddagger_3 , i.e.,

(21) Yu, H.-G.; Muckerman, J. T. *J. Phys. Chem. A* **2005**, *109*, 1890.

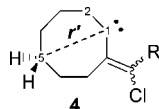


FIGURE 10. Definition of r' for the calculation of the reaction $4 \rightarrow 5$ (at B3LYP/6-31G*).

$4 \rightarrow \ddagger_3 \rightarrow 5$, failed. Hence, we carefully probed the $4 \rightarrow 5$ reaction path by decreasing the distance, r' , between C₁ and C₅ (Figure 10) from 3.5 to 1.5 Å in 0.1-Å increments.¹⁷ Computation of the $4 \rightarrow 5$ reaction path in this manner revealed a shallow intermediate, $4'$. At B3LYP/6-31G*, carbene $4'$ is a more stable conformational isomer of 4 , from which the barrier to C–H insertion (to yield 5) is nearly zero: $E_{a(4' \rightarrow 5)} = 0.3\text{--}0.7$ kcal/mol via \ddagger_3 .

Completing the calculation of the proposed mechanism in Scheme 2 for the phenylchloro case at B3LYP/6-31G*, insertion of the carbene center of *E*-4-PhCl into a phenyl C–H bond is also possible and is indeed viable. Transition state \ddagger_4 was computed for *E*-4-PhCl \rightarrow 6-PhCl ($E_a = 1.9$ kcal/mol; Scheme 8S, Supporting Information), followed by rearrangement to aromatic 7-PhCl via \ddagger_5 with $E_a = 7.4$ kcal/mol.²²

Conclusions

Dichloro- and phenylchlorocarbene (CCl₂ and PhCCl) add to cyclooctyne (**1**) in a concerted, asynchronous manner without any activation barriers. The major product of **1** + RCCl (R = Cl, Ph) is cyclopropene adduct **3**. An alternative **1** + RCCl addition pathway to produce vinyl carbene **4** may result from dynamic control of the system. However, if **4** is formed at all, we believe it will be very short-lived, readily rearranging to **3**, or via transannular C–H insertion to ultimately form bicyclo-[3.3.0]octane derivative **5**; the activation energies for these two processes are less than 8 kcal/mol. If reaction dynamics do control chlorocarbene–cyclooctyne additions, we believe that most of the reactions occur by traditional carbene cycloaddition, and nominal amounts of products formed via the alternative route though carbene **4**.

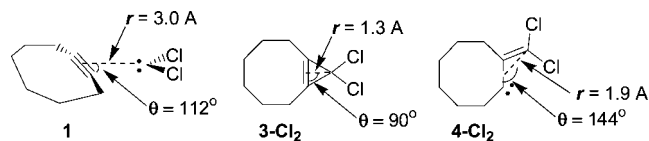
In addition to completing the experimental investigations of CX₂ and PhCX additions to cyclooctyne (X = Cl, Br), in the future we intend to run trajectories of **1** + CCl₂ to determine the role, if any, that reaction dynamics play in controlling this reaction, at least in the gas phase.

Computational Methods. Gas-phase calculations were performed with Gaussian 98²³ or Gaussian 03.²⁴ Stationary points were confirmed by frequency calculations: energy minima had all real frequencies, and transition states were confirmed by the presence of one imaginary frequency. The PESs of carbene additions to cyclooctyne (**1**) were calculated at B3LYP/6-311+G*^{25,26} and MP2/6-311+G*^{26,27} for dichlorocarbene (CCl₂) and at B3LYP/6-31G* for phenylchlorocarbene (PhCCl) (Figures 8 and 9, respectively). Quadratic synchronous transit methods were used to find transition states unless otherwise noted, and energies were ZPE-corrected, scaling by 0.9826.¹⁶

Calculations for the addition of CCl₂ to **1** were performed with approach of CCl₂ endo (from the top) and exo (from the side) to **1** at distances of r , where r is the length of the carbene carbon to the center of the triple bond of **1** (Figure 1), as per

(22) Reaction of *Z*-4-PhCl \rightarrow 6-PhCl via phenyl C–H insertion was not considered due to the unfavorable stereochemistry of the phenyl ring in relation to the carbene center in *Z*-4-PhCl.

previous calculations of alkene–CCl₂ additions.^{1,2,14} Structures were optimized at $r = 1.1\text{--}3.5$ Å in 0.1-Å increments at B3LYP/6-311+G* and MP2/6-311+G*. The resulting reaction coordinates, E_{rel} vs r , are shown in Figure 2. Given that endo and exo approaches of CCl₂ to **1** yielded the same results (Supporting Information, Figure S1), only endo addition of PhCCl to **1** was calculated. The same methods used for **1** + CCl₂ were utilized for PhCCl (Figure 4), except at B3LYP/6-31G*.



To investigate the possibility that **1** + CCl₂ may produce carbene **4-Cl₂** we computed a three-dimensional PES at B3LYP/6-31G*. B3LYP/6-31G* was selected because it provided results comparable to those obtained with a larger basis set and at the MP2 level of theory (cf. Figure 2). We defined two appropriate coordinates for the PES: the distance, r , between the carbene center and center of the cyclooctyne π system (as previously) and angle, θ , from the carbene center to the midpoint of the cyclooctyne triple bond to one of the alkynyl carbons. The former coordinate decreases from effective infinity to ~ 1.3 Å in cyclopropene **3** and ~ 1.9 Å in carbene **4**. The angle coordinate begins at a value of 112° for the separated cyclooctyne and CCl₂, and decreases to 90° in **3**, and expands to 144° in **4**. For these PES calculations, $r = 1.2\text{--}3.0$ Å in 0.2 Å increments and $\theta = 90\text{--}150^\circ$, in 5° increments. Figure 5 shows the resulting 3D PES.

To probe further the possible reaction of **1** + CCl₂ \rightarrow **4-Cl₂**, we calculated a reaction coordinate using a constant carbene

(23) Frisch, M. J.; Trucks, G. W.; Schlegel, H. B.; Scuseria, G. E.; Robb, M. A.; Cheeseman, J. R.; Zakrzewski, V. G.; Montgomery, J. A.; Stratmann, R. E.; Burant, J. C.; Dapprich, S.; Millam, J. M.; Daniels, A. D.; Kudin, K. N.; Strain, M. C.; Farkas, O.; Tomasi, J.; Barone, V.; Cossi, M.; Cammi, R.; Mennucci, B.; Pomelli, C.; Adamo, C.; Clifford, S.; Ochterski, J.; Petersson, G. A.; Ayala, P. Y.; Cui, Q.; Morokuma, K.; Malick, D. K.; Rabuck, A. C.; Raghavachari, K.; Foresman, J. B.; Cioslowski, J.; Ortiz, J. V.; Stefanov, B. B.; Liu, G.; Liashenko, A.; Piskorz, P.; Komaromi, I.; Gomperts, R.; Martin, R. L.; Fox, D. J.; Keith, T.; Al-Laham, M. A.; Peng, C. Y.; Nanayakkara, A.; Gonzalez, C.; Challacombe, M.; Gill, P. M. W.; Johnson, B. G.; Chen, W.; Wong, M. W.; Andres, J. L.; Head-Gordon, M.; Replogle, E. S.; Pople, J. A. *Gaussian 98, Revision A.11*; Gaussian, Inc.: Pittsburgh, PA, 2001.

(24) Frisch, M. J.; Trucks, G. W.; Schlegel, H. B.; Scuseria, G. E.; Robb, M. A.; Cheeseman, J. R.; Montgomery, J. A., Jr.; Vreven, T.; Kudin, K. N.; Burant, J. C.; Millam, J. M.; Iyengar, S. S.; Tomasi, J.; Barone, V.; Mennucci, B.; Cossi, M.; Scalmani, G.; Rega, N.; Petersson, G. A.; Nakatsuji, H.; Hada, M.; Ehara, M.; Toyota, K.; Fukuda, R.; Hasegawa, J.; Ishida, M.; Nakajima, T.; Honda, Y.; Kitao, O.; Nakai, H.; Klene, M.; Li, X.; Knox, J. E.; Hratchian, H. P.; Cross, J. B.; Adamo, C.; Jaramillo, J.; Gomperts, R.; Stratmann, R. E.; Yazyev, O.; Austin, A. J.; Cammi, R.; Pomelli, C.; Ochterski, J. W.; Ayala, P. Y.; Morokuma, K.; Voth, G. A.; Salvador, P.; Dannenberg, J. J.; Zakrzewski, V. G.; Dapprich, S.; Daniels, A. D.; Strain, M. C.; Farkas, O.; Malick, D. K.; Rabuck, A. D.; Raghavachari, K.; Foresman, J. B.; Ortiz, J. V.; Cui, Q.; Baboul, A. G.; Clifford, S.; Cioslowski, J.; Stefanov, B. B.; Liu, G.; Liashenko, A.; Piskorz, P.; Komaromi, I.; Martin, R. L.; Fox, D. J.; Keith, T.; Al-Laham, M. A.; Peng, C. Y.; Nanayakkara, A.; Challacombe, M.; Gill, P. M. W.; Johnson, B.; Chen, W.; Wong, M. W.; Gonzalez, C.; Pople, J. A. *Gaussian 03, Revision B.04*; Gaussian, Inc.: Pittsburgh, PA, 2003.

(25) (a) Lee, C.; Wang, W.; Parr, R. G. *Phys. Rev. B* **1988**, *37*, 785. (b) Becke, A. D. *Phys. Rev. A* **1988**, *38*, 3098. (c) Becke, A. D. *J. Chem. Phys.* **1993**, *98*, 5648.

(26) Recent calculations on CCl₂ have utilized diffuse functions to increase computational accuracy. In these papers, similar results were obtained with B3LYP/6-311+G(d) and 6-311+G(3d,f), MP2/6-311+G*, and CCSD(T)/6-311+G* (ref 26a), and B3LYP/6-311++G** and MP2/6-31G(d) (ref 26b): (a) Kong, Q.; Wulff, M.; Bratos, S.; Vuilleumier, R.; Kim, J.; Ihee, H. *J. Phys. Chem. A* **2006**, *110*, 11178–11187. (b) Singleton, D. A.; Wang, Z. *Tetrahedron Lett.* **2006**, *46*, 2033–2036.

approach angle of $\phi = 143^\circ$ and varied distances of r (Figure 6). Distance r was defined as above, and the value of ϕ was selected because the corresponding angle in carbene **4-Cl₂** is 143° . Again, structures were optimized at $r = 1.1\text{--}3.5$ Å in 0.1 Å increments at HF/6-31G*, maintaining constant angle $\phi = 143^\circ$. The resulting reaction coordinate, E_{rel} vs r with a constant carbene approach angle of 143° is provided as Figure S2 in the Supporting Information.

The reaction coordinate for the reverse reaction **4-Cl₂** \rightarrow $\ddot{\text{C}}_1' \rightarrow$ **1** + CCl₂ was computed by stretching the C=C alkene bond of **4-Cl₂** from 1.35 to 2.1 Å in 0.1 -Å increments at B3LYP/6-31G*. The reaction coordinate was then graphed as E_{rel} vs r , with the C=C lengths converted to carbene-center-to-alkyne distances r , as defined above; it is included as Figure S3 in the Supporting Information. The reaction path of **4** \rightarrow $\ddot{\text{C}}_3 \rightarrow$ **4'** \rightarrow $\ddot{\text{C}}_3' \rightarrow$ **5** was calculated in a similar "stepwise" manner at B3LYP/6-31G*. Distance r' between C₁ and C₅ (Figure 10) was shortened from 3.5 to 1.5 Å in 0.1 Å increments. The **4** \rightarrow **4'** \rightarrow **5** reaction coordinate is provided as Figure S4 in the Supporting Information as well.

Acknowledgment. We thank the NSF (CHE-0517876), PRF (37969-GB4), Research Corporation (CC5551), and Barnard College for financial support. X.Y.M. is grateful for a Barry

M. Goldwater Scholarship and for a Bernice Segal Fellowship from the Barnard Chemistry Department. S.E.B. thanks the Barnard Chemistry Department for a Bernice Segal Fellowship and the Office of the Dean of Students of Barnard College for additional support. We thank Denise Napolitano, Kaitlyn Suski, and Jennifer Schloss for their experimental work on this project thus far. D.C.M. thanks Professors Dean Tantillo, Jeehiun Lee, and Lawrence Scott for helpful discussions and suggestions. We are also grateful to Esther Blue and Deepak Mishra for invaluable technical support. We also acknowledge helpful suggestions from reviewers.

Supporting Information Available: Table of relative electronic energies for the stationary points in Figures 8 and 9; calculated reaction coordinates for **1** + CCl₂ \rightarrow **4-Cl₂**, **4-Cl** \rightarrow $\ddot{\text{C}}_1' \rightarrow$ **1** + CCl₂, and **4** \rightarrow **4'** \rightarrow **5**; Cartesian coordinates and imaginary frequencies (where applicable) of all stationary points. This material is available free of charge via the Internet at <http://pubs.acs.org>.

JO801736X

(27) (a) Möller, C.; Plesset, M. S. *Phys. Rev.* **1934**, *46*, 618–622. (b) Leininger, M. L.; Allen, W. D.; Schaefer, H. F.; Sherrill, C. D. *J. Chem. Phys.* **2000**, *112*, 9213–9222.